








RESEARCH ARTICLE | DECEMBER 01 2023

Fiber-based broadband detection of a rotational object with superposed vortices

Ziyi Tang ; Zhenyu Wan ; Han Cao ; Yize Liang ; Wei Zhou; Yuchen Zhang ; Liang Fang ; Jian Wang  



APL Photonics 8, 126101 (2023)

<https://doi.org/10.1063/5.0167478>

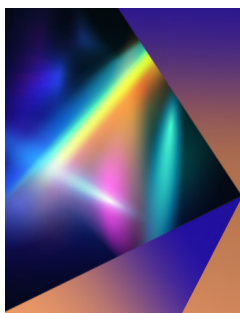


View
Online



Export
Citation

CrossMark



APL Photonics

Applications Now Open for the
Early Career Editorial Advisory Board

[Learn more and submit!](#)

Fiber-based broadband detection of a rotational object with superposed vortices

Cite as: APL Photon. 8, 126101 (2023); doi: 10.1063/5.0167478
Submitted: 13 July 2023 • Accepted: 9 November 2023 •
Published Online: 1 December 2023



Ziyi Tang,^{1,2} Zhenyu Wan,^{1,2,3} Han Cao,^{1,2} Yize Liang,^{1,2} Wei Zhou,^{1,2} Yuchen Zhang,^{1,2}
Liang Fang,^{1,2} and Jian Wang^{1,2,a)}

AFFILIATIONS

¹ Wuhan National Laboratory for Optoelectronics and School of Optical and Electronic Information, Huazhong University of Science and Technology, Wuhan 430074, Hubei, China

² Optics Valley Laboratory, Hubei, Wuhan 430074, China

³ School of Physics and Astronomy, University of Glasgow, Glasgow G12 8QQ, United Kingdom

^{a)} Author to whom correspondence should be addressed: jwang@hust.edu.cn

ABSTRACT

Recently, the rotational Doppler effect has attracted broad attention in detecting rotational motion. However, the presently proposed detection techniques based on the rotational Doppler effect are generally configured relying on discrete components in free space, resulting in cumbersome and inflexible systems, which brings challenges to practical applications. In this paper, we demonstrate a fiber-based configuration on rotational Doppler measurements for the detection of a rotational object using an ultra-broadband mode-selective coupler to convert the superposed vortices. Remarkably, the results show the broadband operating range of the fiber-based measurement system intuitively through wavelength scanning. The refinement of rotational Doppler detection techniques is of great significance for lowering the cost, reducing system complexity, improving system integration, and industrial manufacturing. This fiber-based scheme might be a promising candidate for facilitating the rotational Doppler effect applied as novel motion monitoring and sensing equipment in engineering and industry.

© 2023 Author(s). All article content, except where otherwise noted, is licensed under a Creative Commons Attribution (CC BY) license (<http://creativecommons.org/licenses/by/4.0/>). <https://doi.org/10.1063/5.0167478>

I. INTRODUCTION

Since the seminal paper by Yeh and Cummins in 1964,¹ the Doppler effect has exhibited widespread application in velocity detection among diverse scenarios from scientific research to engineering, on account of the advantages of noninvasive nature, fast dynamic response, and high accuracy.^{2–4} In earlier studies, without the consideration of the physical dimensions of the light field, the Doppler effect once mainly described the frequency shift of waves caused by the translational motion between the observer and the source. As well known, in addition to the typical plane wave, the wave can also take the form of a special spatial topological distribution, such as the vortex beam, which was recognized by Allen *et al.* in 1992 as carrying an orbital angular momentum (OAM),⁵ enabling more abundant controllable dimensions beyond the spin counterpart.^{6–10} The vortex beam is characterized by a doughnut-shaped intensity profile and a helical phase front, resulting in an azimuthal component of the Poynting vector in free space.^{11–13} In

1998, Courtial *et al.* first observed the Doppler shift imparted to a mm-wave beam with an OAM in the experiment,¹⁴ which is now known as the rotational Doppler effect.¹⁵ Since then, the rotational Doppler effect has extensively been studied in its origin and theoretical model for various objects, such as rotating beams, small particles, and rough surfaces.^{16–20} In particular, this new type of Doppler effect has attracted broad attention in numerous fields, including acoustics,^{21–23} optics,^{24–29} and electromagnetics.^{30–32}

One can relate the frequency shift of light to the rotational motion of objects using the properties of the rotational Doppler effect and benefiting from the characteristics of optical vortices. In 2013, a pioneering study by Lavery *et al.* first demonstrated the detection of a spinning rough surface using superposed vortex beams,³³ revealing the significance of the rotational Doppler effect in rotational speed measurements, where the superimposed vortex beam refers to the superposition of two beams with different OAMs, especially carrying opposite topological charges, which would form petal-like fringes. Subsequently, Rosales-Guzmán and

his colleagues reported a series of studies on the detection of rotating small particles by means of an interferometric setup.^{34–36} At the technical level, the self-mixing interference scheme, the interference within the laser between feedback light carrying external object information and intracavity light, has been employed to extract the rotational Doppler shift for speed measurements.^{37,38} In particular, Qiu *et al.* analyzed, in detail, the influence of lateral displacement (transverse misalignment between the optical axis and the rotation center) and angular deflection (inclination between the optical axis and the motion plane normal) during the measurement process.^{39,40} As a further refinement, rotation direction discrimination is implemented by introducing additional physical dimensions of the light field.^{41,42} In addition, the rotational Doppler effect has also been investigated on many occasions, such as detecting angular acceleration,⁴³ measuring flow vorticity,^{44,45} observing optically trapped microspheres,^{46,47} remote sensing,^{48–50} and incoherent light detection.⁵¹

At present, the speed measurement devices based on the rotational Doppler effect are generally constructed relying on discrete components in free space, which means that the entire process from the generation and transmission of probe light to the transmission of scattered signal light after being collected is considered to take place in free space. Nevertheless, the complex components of the optical paths in free space cause the system to be too cumbersome and inflexible, making it hard to be applied in real engineering scenarios. Similar to this situation, the development of conventional laser Doppler velocimeters has undergone a transition from a free-space architecture to a fiber-based architecture. As known, optical fibers are an excellent transmission medium for light fields; they have unique properties, such as low loss, small size, lightweight, and bending resistance. As a result, they are now employed in a wide range of sensing and measuring equipment, especially in commercial Doppler velocimeters, where the fiber-based architecture is often more competitive in cost than the free-space architecture.⁵² In our previous work, we have demonstrated the advantages of optical fibers as the transmission medium for probe light due to the great flexibility of optical paths and the high efficiency of long-distance transmission.⁵³ However, the probe light is still generated through a spatial light modulator (SLM) in free space, and thus, the overall compactness of the measuring system needs to be further improved. It is worth noting that the superposed vortex mode with opposite helicity of the light field, in optical fibers, is equivalent to an eigenmode in weakly guiding fibers, the linearly polarized (LP) mode. Fortunately, there are several ways to directly control the modes in optical fibers,^{54–56} providing suitable fiber-based elements for optical field modulation that are essential during speed measurement.

In this paper, a fiber-based configuration, utilizing rotational Doppler measurements, is reported for detecting rotation. We construct a compact and flexible velocimeter using fiber components, by building an ultra-broadband mode-selective coupler (MSC) with controlling LP mode to excite superposed vortices. We designed several MSCs to create LP modes individually from LP₁₁ to LP₅₁, respectively. The results show that when a rotating rough surface is illuminated by the probe light with $\pm n$ -order ($n = 1–5$) superposed vortices, the Doppler beat frequency of the scattered signal light arises with a linear relationship $2n$ times as the rotational speed. Furthermore, we experimentally demonstrate the achromatic property of the rotational Doppler effect intuitively, through

wavelength scanning covering the S-, C-, and L-bands for the broadband detection of the rotating rough surface. The proposed velocimeter is insensitive to variations in the wavelength of the light source, which is conducive to the detection of transparent materials at certain wavebands, and, thus, is of great significance for lowering the cost. This fiber-based method is a promising candidate for utilizing the rotational Doppler effect in practical applications, such as motion monitoring and sensing equipment.

II. THEORY AND CONCEPT

A. Rotational Doppler effect induced by vortex beam

The intrinsic feature of the Doppler effect describes the frequency shift of a wave that arises from the relative motion between a source and an observer. The rotational Doppler effect and the conventional linear Doppler effect, in essence, share a common origin.¹⁹ In other words, the mechanism by which the rotational Doppler shift is induced can be derived from the classical analysis method of the well-known linear Doppler effect. With this perspective, we consider the interaction between a rotating rough surface and a vortex beam with a single helical phase structure. When viewed from a certain position on the rotating rough surface, the lateral movement in the local position is equivalent to an instantaneous linear velocity as

$$\vec{v}_\phi = \Omega r \cdot \vec{e}_\phi, \quad (1)$$

where \vec{e}_ϕ represents the azimuth vector in polar coordinates, r and ϕ are the radius and azimuthal angle of the local position, respectively, and Ω is the angular velocity of the rotating rough surface. Note that there is a tiny inclination between the Poynting vector of the vortex beam and its beam axis as $\alpha = \ell/rk$,⁵⁷ where ℓ is the helicity of the transverse phase during a cycle, r is the radius from the beam axis, and k is the wavenumber of light. Assuming that a ℓ_1 -order vortex beam is illuminating the rough surface with normal incidence and the beam axis is aligned with the rotation axis, the azimuth projection of the Poynting vector of the incident light corresponding to the local position of the rough surface is given as

$$\vec{k}_{\ell_1, \phi} = \sin \alpha \cdot k \vec{e}_\phi \approx \frac{\ell_1}{r} \vec{e}_\phi, \quad (2)$$

where the approximation is used at a small angle. In general, the scattering of incident light from the rough surface is a random process, which means that the scattered light can be decomposed into a sum of components with different vortex modes. For the ℓ_0 -order vortex component, the azimuth projection of its Poynting vector is similarly written as $\vec{k}_{\ell_0, \phi} \approx \ell_0/r \cdot \vec{e}_\phi$.

According to wave optics theory, the linear Doppler shift occurs when the wave vector difference $\Delta \vec{k}$ between the incident and scattered light is not orthogonal to the velocity vector \vec{v} . It can be represented as $\Delta f_v = \Delta \vec{k} \cdot \vec{v} / 2\pi$. Obviously, for the rotational Doppler effect, the change in the skew Poynting vector at each position where the vortex beam interacts with the rough surface will also induce a similar frequency shift. As a result, with regard to a certain vortex component in the scattered light from the rough surface, its rotational Doppler shift can be expressed as

$$\Delta f_{\ell_1, \ell_0, \Omega} = \frac{1}{2\pi} \left(\vec{k}_{\ell_1, \phi} - \vec{k}_{\ell_0, \phi} \right) \cdot \vec{v}_\phi = \frac{(\ell_1 - \ell_0)\Omega}{2\pi}. \quad (3)$$

Hence, when a vortex beam illuminates a rotating rough surface, the scattered light will be modulated with a frequency shift, which is related to the difference in helicity of the modes in the incident and scattered light, as well as the angular velocity.

B. Detection technique of rotational Doppler shift with superposed vortices

The rotational motion of an object can be detected by means of the rotational Doppler shift. However, in laser surface velocimetry, the optical beat technique is crucial in extracting the Doppler shift because it is difficult to sense optical frequencies directly by existing detectors. One of the established detection techniques of rotational Doppler shift is the so-called fringe type.⁵⁸ This means that the target is illuminated by a superposed vortex mode with opposite helicity, forming a petal pattern of azimuthal fringes. Obviously, such a beam is equivalent to the LP mode in terms of intensity characteristics. Meanwhile, the eigenmodes in optical fibers can form a set of orthogonal bases, i.e., different groups of modes can be converted to each other by orthogonal mapping. Typically, the LP mode can be converted into a linear superposition of vortex modes with opposite topological charges. As a result, when a ℓ -order LP mode illuminates the rough surface, there will be two rotational Doppler shifts induced, corresponding to the two components of the vortex modes, i.e., $\Delta f_{\pm\ell\ell_0,\Omega} = (\pm\ell - \ell_0)\Omega/2\pi$ for the ℓ_0 -order scattered mode. Scattered signal light collected in any mode will thus contain components that have experienced different Doppler shifts by virtue of the different illumination directions of the two skew Poynting vectors. Considering their superposition on the photodetector (PD), the beat frequency obtained is given by

$$|\Delta f_{\ell,\Omega}| = |\Delta f_{+\ell\ell_0,\Omega} - \Delta f_{-\ell\ell_0,\Omega}| = \frac{\ell\Omega}{\pi}. \tag{4}$$

Intuitively, the beat frequency of the scattered signal light is exactly proportional to the product of the LP mode order in the probe light and the angular velocity. This is key to detecting rotation. In addition, each individual mode in the scattered light shares the same

beat frequency. This means that although the scattered modes are mixed together in a complex manner, a clear Doppler peak can still be obtained directly in the signal spectrum of a detected mode. One can clearly see from Eqs. (3) and (4) that neither the rotational Doppler shift nor the detected beat frequency is dependent on the wavelength. In other words, one striking feature of the rotational Doppler effect is achromatic with respect to the wavelength of the light source, as demonstrated by Lavery *et al.*⁵⁹

C. Concept of fiber-based rotational Doppler measurements

In this work, as shown in Fig. 1, the probe path and the detection path are configured and connected to two ports by fiber-based components, respectively. On the probe path, the LP_{n1} ($n = 1-5$) modes are converted individually from the LP₀₁ mode by a fiber-based controller and then output from port 1 as the probe light after transmission through the multi-mode fiber (MMF). Here, the LP mode controller can work in an ultra-broadband spectrum, enabling wavelength scanning operations. According to the above-mentioned analysis, the probe light can be regarded as containing two components with $\pm n$ -order superposed vortices. After being collimated out into free space, the probe light illuminates the rotating rough surface at a small incidence angle. A set of complex vortex modes, carrying the rotational Doppler shifts, is scattered from the rough surface. On the detection path, the scattered light is collected into an MMF by the mode filtering action of it. The Gaussian mode is coupled most effectively, and its beat frequency $|\Delta f_{\Omega}|$ is obtained by the detector. According to Eq. (4), once the beat frequency is extracted, the angular velocity of the rotating rough surface can be deduced as $\Omega = \pi \cdot |\Delta f_{\Omega}|/n$. The steps to achieve rotation detection can be summarized as follows: First, the Gaussian beam output by laser is converted into a higher-order mode through a fiber-based controller; next, the high-order mode beams illuminate the rotating rough surface; then, the rough surface scatters complex vortex modes of light; and finally, the scattered light is collected by the

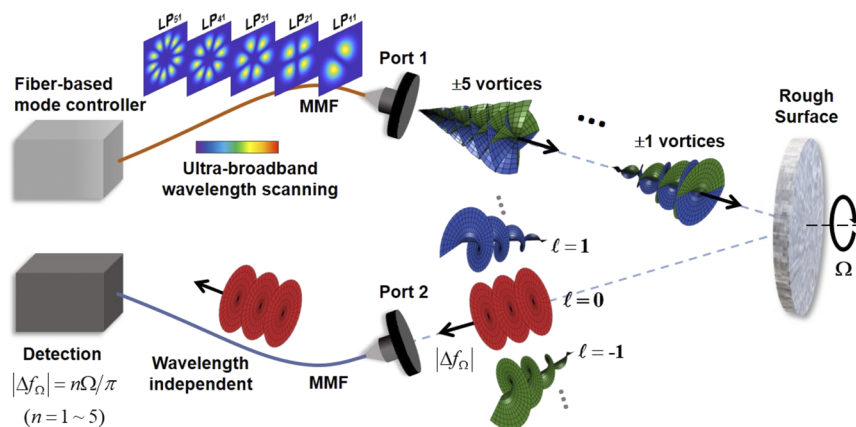


FIG. 1. Concept of fiber-based rotational Doppler measurements for a rotating object. The LP_{n1} ($n = 1-5$) mode launched by a fiber-based controller illuminates the rough surface from port 1, and the scattered light carrying the rotational Doppler shift is collected from port 2 into the multi-mode fiber (MMF) for detection. The detection is wavelength-independent under ultra-broadband scanning.

MMF and its frequency shift is extracted to calculate the rotational speed.

In this case, the probe light illuminates the rough surface with oblique incidence. Although strictly the rotational Doppler shift of oblique incident light broadens into many peaks around the original value,³⁹ the maximum peak remains constant at a small incident angle, and thus, the influence of this on the measurement can be ignored. In addition, the rotational Doppler effect is wavelength-independent, and thus, the detection results will not be affected by the wavelength drift of the light source. In a sense, the achromatic property is beneficial to the cost-effectiveness of the fiber-based rotational Doppler measurement. For example, the wavelength calibration of the laser source during velocimetry is no longer troubling, which will greatly reduce the maintenance cost of the equipment.

III. EXPERIMENTAL SETUP

Based on the principle described in Fig. 1, the experimental scheme follows the optical fiber composition of the mode controller and the ports of the probe and the receiver. The experimental setup is constructed with fiber-based components for detecting the angular velocity of a rotating rough surface based on the rotational Doppler effect, as illustrated in Fig. 2. The laser with an output power of 10 mW is employed to launch a Gaussian beam, i.e., the LP₀₁ mode in a single-mode fiber (SMF). In particular, the experiments were carried out with three types of laser sources, respectively, to investigate the dependence of the measuring system on wavelength and linewidth, including a narrow linewidth tunable laser (Santec, TSL-550), a broadband laser (Amonics, ALS-CL-15-B-FA), and a distributed feedback (DFB) laser. An MSC, in which the input end is connected to a SMF and the output end is connected to a multi-mode fiber (MMF), is used to control the mode. In particular, for the higher-order LP_{*n*} mode (*n* > 1), a ring-core fiber (RCF) is fused to the output of the MMF to filter out the mixed modes caused by crosstalk in the MMF. By properly adjusting the two polarization controllers (PC1 and PC2), the LP₀₁ mode in SMF is converted to the LP_{*n*} mode in MMF with high efficiency. After output from the MMF, the LP_{*n*} mode is collimated by a collimator (Col. 1) and illuminates the rough surface at a small angle of incidence. The rough surface is a piece of tinfoil pasted on a hard board, which is driven to rotate by a high-speed rotor. The beam center of the probe light is aligned with the rotational center of the rough surface by

precisely adjusting the azimuth dimension of Col. 1. Subsequently, another collimator (Col. 2), placed next to Col. 1, is utilized to collect the scattered light. The scattered light is then coupled into the MMF, in which the Gaussian mode gets a higher coupling efficiency than other scattering modes. In addition, the high-order modes will also be greatly filtered out during the transmission in MMF. Therefore, the Gaussian mode dominates the signal light received by the photodetector (PD). The electrical signal converted by the PD is transmitted to the oscilloscope via a cable for signal display and processing. In data collection, the signal acquisition window in the time domain is 1 s, giving the frequency resolution in the fast Fourier transform (FFT) analysis of 1 Hz. In signal processing, the Doppler peak is searched in the Fourier amplitude spectrum, and the corresponding frequency value is recorded as the beat frequency $|\Delta f_0|$ of the rotational Doppler shifts. As a result, the magnitude of the rotational speed of the rough surface is obtained by calculation.

Generally, there are several alternative techniques for mode controlling through the fiber-based element, such as asymmetric grating and fiber grating. Nevertheless, an MSC, similar to what we designed before,³⁶ is adopted here for its excellent performance in broadband working. The MSC is fabricated with an SMF and an MMF through two steps, including pre-tapering of the SMF and fused tapering of the two fibers. The pre-tapered process is to satisfy the phase-matching condition, and the fused-tapered process is to achieve sufficient coupling between the two fibers by twisting them together and then heating and slowly stretching. In order to improve performance stability under environmental disturbance, the MSC is encapsulated before being connected to the measurement system. For the 1-order MSC, when the LP₀₁ mode is input from the SMF, the LP₁₁ mode is excited in the MMF, as shown in Fig. 3(a). For the higher-order MSC that sculpts LP_{*n*} modes (*n* > 1), an RCF is fused to the output MMF port, as shown in Fig. 3(b). To overcome the inter-mode crosstalk in MMF, the RCF is employed as the mode filter to improve the purity of output LP modes.

As known, there is an equivalence between the LP_{*n*} mode and the $\pm n$ -order superposed vortices, and then, the MSC can be adopted as a probe light generator in rotational Doppler measurements, resulting in a compact structure. We design five types of MSC for generating different orders of vortex light. The effective refractive index of different modes in the SMF (LP₀₁) and MMF (LP₀₁, LP₁₁, LP₂₁, LP₃₁, LP₄₁, and LP₅₁) as a function of the radius of fiber is calculated as shown in Fig. 3(c), and the insets are the experimentally obtained intensity profiles of the converted LP_{*n*} modes

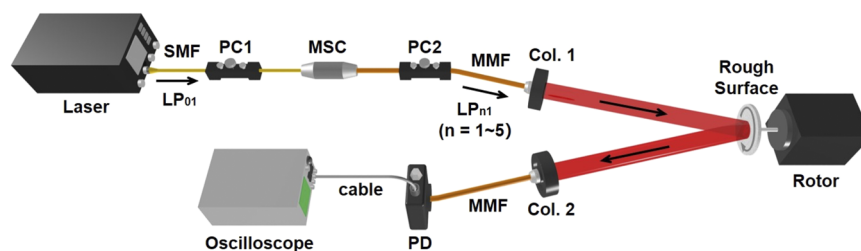


FIG. 2. Experimental setup. SMF: single-mode fiber; PC1 and PC2: polarization controllers; MSC: mode-selective coupler; MMF: multi-mode fiber; Col. 1 and Col. 2: collimators; and PD: photodetector.

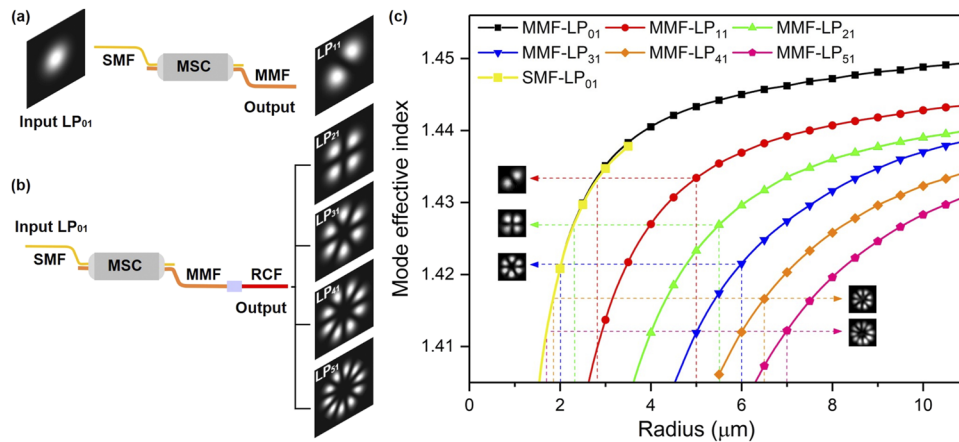


FIG. 3. Structure of the MSC. (a) The structure schematic of the 1-order MSC. (b) The structure schematic of the higher-order MSC. (c) The effective refractive index of different modes in the SMF (LP_{01}) and MMF (LP_{01} , LP_{11} , LP_{21} , LP_{31} , LP_{41} , and LP_{51}) as a function of the tapered radius of the fiber.

with a fabricated MSC. It can be seen that the mode effective refractive index decreases with the tapering fiber core. In the design of the coupler, it is required to match the effective refractive index between the LP_{01} mode in the SMF and the LP_{n1} mode in the MMF to satisfy the phase-matching condition. Under the same effective refractive index, the higher the order of LP mode, the larger the core radius. This means that the length of the pre-tapering designed for

the fabrication of the higher-order MSC will be longer. There are five phase-matching points selected for simulations, in which each dotted line represents the fiber dimensions corresponding to the LP_{n1} ($n = 1-5$) mode, respectively. By experimentally adjusting the coupling efficiency, the desired mode and the light-splitting ratio could be attained. The lengths of the fiber pre-tapering are designed as 3.9 mm for LP_{11} mode, 7.9 mm for LP_{21} mode, 12.3 mm for LP_{31}

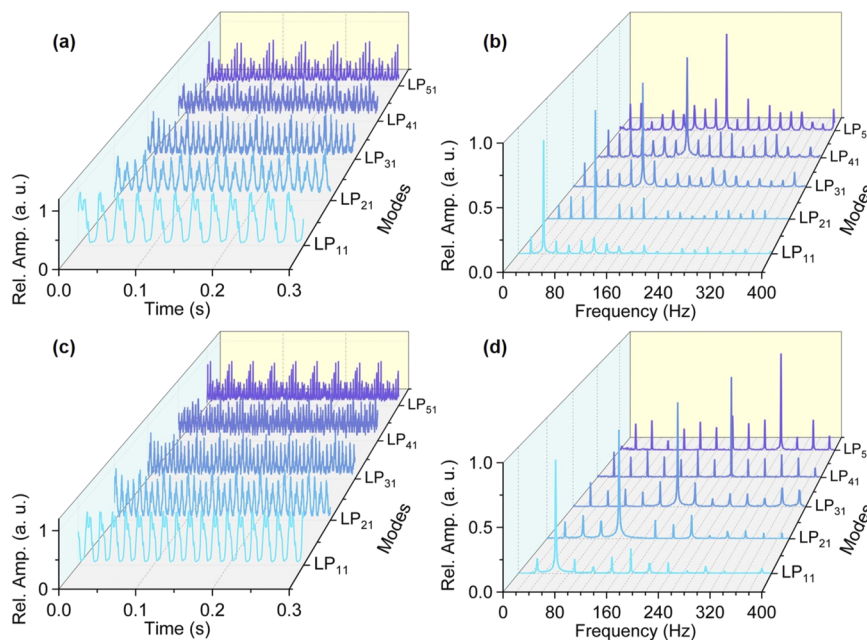


FIG. 4. The typical results for detecting the rotating rough surface. (a) and (b) The time-domain intensity signals and Fourier spectra of detected signals of different LP modes under the angular velocity of 40π rad/s, respectively. (c) and (d) The time-domain intensity signals and Fourier spectra of detected signals of different LP modes under the angular velocity of 60π rad/s, respectively.

mode, 16.7 mm for LP₄₁ mode, and 20.5 mm for LP₅₁ mode, and they determine the respective suitable fiber dimensions during the coupling process.

IV. RESULTS

At the first step of experimental demonstration, the narrow linewidth tunable laser is set at a wavelength of 1550 nm to detect the rotating rough surface. At the angular velocities of 40π and 60π rad/s, respectively, the measured time-domain intensity signals and the corresponding Fourier spectra are shown in Fig. 4. At each angular velocity, the MSC of different orders is switched to generate different LP modes, including LP₁₁ to LP₅₁, in the experiment. Clearly, the time-domain signals show the periodic variation in the trigonometric function and the period changes with the rotational speed and the order of LP modes. In addition, at the angular velocity of 40π rad/s, there are some distinct Doppler peaks, respectively, in five Fourier spectra from 40 to 200 Hz at intervals of 40 Hz corresponding to different orders of LP₁₁ to LP₅₁ modes. For the angular velocity of 60π rad/s, Doppler peaks range from 60 to 300 Hz at intervals of 60 Hz corresponding to five orders. In Fig. 4, the dominant frequency shift is linear to the rotational speed and the order of LP modes. A higher order or faster rotation would give rise to a greater beat frequency. It is worth noting that each Fourier spectrum has another obvious feature, i.e., there are a series of harmonic peaks around the highest Doppler peak with uniform spacing, and they are also related to the rotational speed. These harmonic peaks mainly arise from the following: On the one hand, according to the modal expansion theory,¹⁸ the scattered light from the rough surface may contain a wide variety of mode components, of which each causes a different rotational Doppler shift. On the other hand, the misalignment of the illuminated probe light in the operation, including a lateral displacement and an angular deflection, may also expand the original Doppler peak into a set of discrete peaks. Although the Gaussian mode will be coupled and transmitted maximally at the detection port, the higher-order modes will still be detected to some extent after low collection efficiency and high loss. As a result, the Doppler peak of the Gaussian mode can still stand out from other peaks.

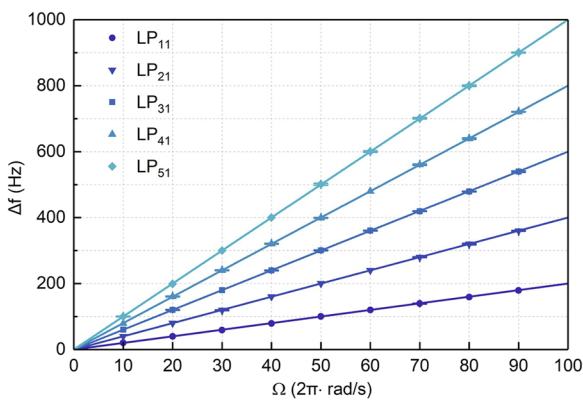


FIG. 5. The measured beat frequencies via different angular velocities at 1550 nm probe light for LP₁₁ to LP₅₁ modes.

In addition, we have also presented the measurement results at the same wavelength for five LP modes by varying the angular velocity of the rotating rough surface from 20π to 180π rad/s, as shown in Fig. 5. At each angular velocity, we take seven measured results for data averaging. The results indicate that for the LP_{n1} (n = 1–5) modes, the measured beat frequencies are 2n times the rotational frequency of the rough surface, which is in line with theoretical expectations. Therefore, the successful implementation of a fiber-based rotational Doppler measurement for detecting a rotating rough surface using ±n-order superposed vortices is demonstrated.

Furthermore, we utilize the tunable laser to test the wavelength dependence of the system through wavelength scanning between 1500 and 1620 nm at 10 nm intervals. At each wavelength, the beat frequency is measured via different angular velocities from 20π to 180π rad/s at 20π rad/s intervals, as shown in Fig. 6(a) where the intensity profiles corresponding to each wavelength are displayed as well. One can clearly see that the beat frequency measured at each wavelength increases linearly with the increase in angular velocity (dots in the same color), and more importantly, the beat frequency measured at different wavelengths maintains exactly the same trend with angular velocity (parallel lines in different colors). This indicates that the demonstrated fiber-based measurement system is wavelength-insensitive within a certain range. As observed by Lavery *et al.*,⁵⁹ the white light backscattered from a rotating object is shifted by a single frequency, i.e., the rotational Doppler

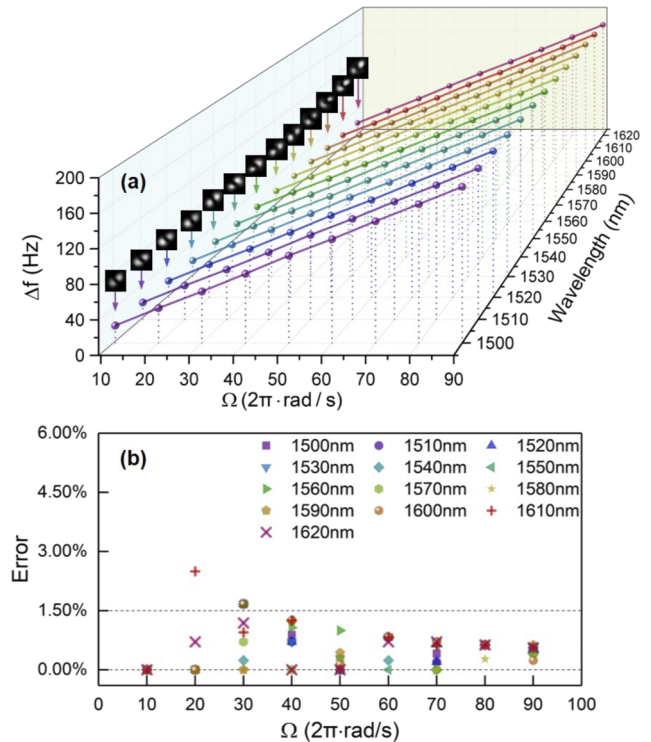


FIG. 6. Measured results via broadband wavelength scanning. (a) The Doppler shifts of variable-speed measurements under wavelength scanning appear as lines of different colors parallel to each other. (b) The measurement error estimation.

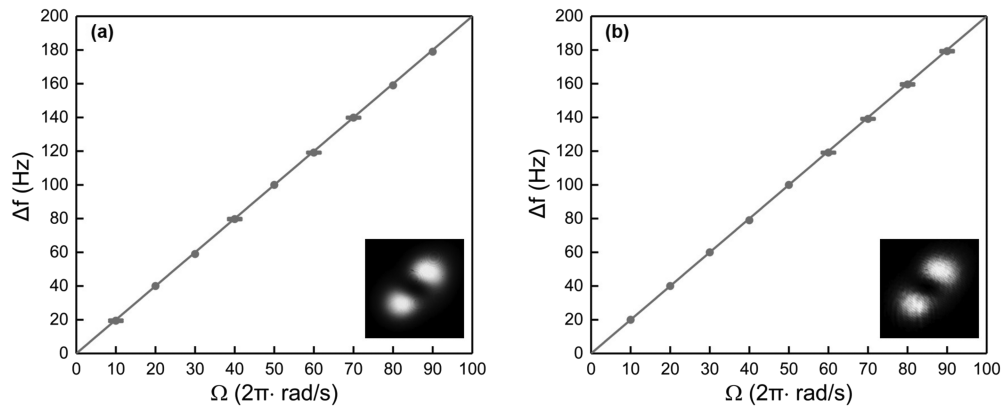


FIG. 7. The measured results via different angular velocities with (a) a broadband laser and (b) a distributed feedback laser. The insets show the intensity profile of the ± 1 -order superposed vortices in both cases.

effect is achromatic. In the experiment, the measurement error estimation is given by the typical standard deviation of seven measurements, as shown in Fig. 6(b). The measured margin of error at each wavelength is almost within 1.5%. This means that the accuracy of the measurement system is not affected by wavelength changes. The measurement precision and accuracy of the fiber-based system mainly depend on the quality of the superposed vortices, which can be further improved by optimizing the performance of the MSC.

To investigate the influence of the laser linewidth on measurements, we also employ a broadband laser source with a wavelength ranging from 1528 to 1608 nm to acquire results, as shown in Fig. 7(a), and take similar operations by a DFB laser with a linewidth of MHz level at 1550 nm, as shown in Fig. 7(b) (the insets show the intensity profiles of the illumination beams). In both cases, we change the angular velocity and record the beat frequency correspondingly. As anticipated, the recorded peak frequency is twice as much as the rotation speed. This indicates that the fiber-based rotational Doppler measurement is independent of the laser linewidth and further verifies the achromatic property of the rotational Doppler shift. Meanwhile, it is of great significance to demonstrate the measurement performance of the system under different laser sources. The test results independent of the technical parameters of the laser just prove that the measurement system has low requirements for light sources. For example, the DFB laser provides a competitive option for integration into the measurement system of commercial applications and presents itself as a mature technique while being relatively cost-effective.

V. DISCUSSIONS AND CONCLUSIONS

The demonstrated fiber-based broadband Doppler measurement of the rotational rough surface shows outstanding operation performance. In the experiment, we adopt a fringe-type technique to perform Doppler measurements using the $\pm n$ -order ($n = 1-5$) superposed vortices as the probe light. Apart from this, in Doppler measurements, there is another technique known as heterodyne-type.⁵⁸ However, the fringe-type technique in our configuration has its distinct advantages. On the one hand, such a detection

technique does not require additional reference light and is thus more highly resistant to environmental disturbance than heterodyne detection; on the other hand, there is still a challenge for heterodyne detection to discriminate the rotational Doppler shift from the overall Doppler effect when the linear and rotational motions exist at the same time although the structured light may provide a potential solution.^{36,60,61} From the technical prospects, the heterodyne detection of the rotational Doppler shift might be abandoned partly with the development of the fringe-type technique for a rotational Doppler velocimeter. For the rotational Doppler velocimeter constructed by free-space discrete components, the system would be too bulky to be integrated. In addition, the discrete components needed to generate optical vortices, e.g., SLM, are costly. To create broadband optical vortices, a prism is considered to compensate for the dispersion of diffractive elements.⁵⁹ As a comparison, in our proposed fiber-based rotational Doppler velocimeter, the mode conversion device is cost-effective, compact, and portable, and more importantly, the MSC can easily achieve an ultra-broadband operating range.

In the experiment, the range of rotational speed we measured is 10–90 revolutions per second (rps), while the extreme range that our system can reach is wider than this. The upper limit of the detection system mainly depends on the response bandwidth of the PD. For example, when a PD with a bandwidth of 6 kHz is employed, the maximum rotational speed that our system can measure is up to 3000 rps, covering the highest speed that motors can reach. The lower limit of the detection system mainly depends on the sampling time and the order of vortex beams. Since higher spectral resolution means a longer sampling time, our measurement requires a quite long sampling time for a low-speed motion, which is unfavorable for real-time monitoring. In our experiments, the time acquisition window length is set to 1 s, so the spectral resolution is 1 Hz, and correspondingly, the minimum detected rotational speed is 0.5 rps for LP₁₁ mode. According to Eq. (4), the acquired beat frequency is proportional to the order of LP mode. Therefore, a high-order LP mode can be utilized as the probe light to optimize the measurement.

In summary, we have proposed and demonstrated a fiber-based Doppler measurement for detecting a rotational object with

controlled LP mode. The constructed system can work in an ultra-broadband spectrum and intuitively exhibits the achromatic property of the rotational Doppler effect. The results show an outstanding performance in terms of rotational speed measurement with errors within 1.5%, and more importantly, this will not be affected by the wavelength and linewidth of the laser source. The significance of this work lies in using a fiber-based configuration, which is conducive to lowering the cost, reducing system complexity, improving system integration, and industrial manufacturing. The fiber-based configuration for rotational Doppler measurements may offer remarkable application prospects in engineering, fluid dynamics, and remote sensing.

ACKNOWLEDGMENTS

We would like to acknowledge Professor Miles J. Padgett at the University of Glasgow for his fruitful discussions.

This work was supported by the National Natural Science Foundation of China (NSFC) (Grant Nos. 62125503 and 62261160388), the Natural Science Foundation of Hubei Province of China (Grant No. 2023AFA028), the Key R&D Program of Hubei Province of China (Grant Nos. 2020BAB001 and 2021BAA024), the Shenzhen Science and Technology Program (Grant No. JCYJ20200109114018750), and the Innovation Project of Optics Valley Laboratory (Grant No. OVL2021BG004).

AUTHOR DECLARATIONS

Conflict of Interest

The authors have no conflicts to disclose.

Author Contributions

Z.T. and Z.W. contributed equally to this work.

Ziyi Tang: Conceptualization (equal); Data curation (equal); Methodology (equal); Validation (equal); Writing – original draft (equal); Writing – review & editing (equal). **Zhenyu Wan:** Conceptualization (equal); Formal analysis (equal); Methodology (equal); Writing – original draft (equal); Writing – review & editing (equal). **Han Cao:** Methodology (supporting); Resources (supporting); Software (supporting). **Yize Liang:** Formal analysis (supporting); Software (supporting). **Wei Zhou:** Resources (supporting); Software (supporting). **Yuchen Zhang:** Investigation (supporting); Methodology (supporting); Software (supporting). **Liang Fang:** Formal analysis (supporting); Investigation (supporting). **Jian Wang:** Conceptualization (equal); Formal analysis (equal); Funding acquisition (lead); Project administration (equal); Resources (equal); Supervision (lead); Writing – review & editing (equal).

DATA AVAILABILITY

Data underlying the results presented in this paper are not publicly available at this time but may be obtained from the corresponding author upon reasonable request.

REFERENCES

- Y. Yeh and H. Z. Cummins, "Localized fluid flow measurements with a He-Ne laser spectrometer," *Appl. Phys. Lett.* **4**, 176–178 (1964).
- O. T. Strand, D. R. Goosman, C. Martinez, T. L. Whitworth, and W. W. Kuhlow, "Compact system for high-speed velocimetry using heterodyne techniques," *Rev. Sci. Instrum.* **77**, 083108.1–083108.8 (2006).
- G. Berkovic and E. Shafir, "Optical methods for distance and displacement measurements," *Adv. Opt. Photonics* **4**, 441–471 (2012).
- A. Donges and R. Noll, *Laser Measurement Technology: Fundamentals and Applications* (Springer, Berlin, Heidelberg, 2015).
- L. Allen, M. W. Beijersbergen, R. J. C. Spreeuw, and J. P. Woerdman, "Orbital angular momentum of light and the transformation of Laguerre-Gaussian laser modes," *Phys. Rev. A* **45**, 8185–8189 (1992).
- K. Y. Bliokh and F. Nori, "Transverse and longitudinal angular momenta of light," *Phys. Rep.* **592**, 1–38 (2015).
- K. Y. Bliokh, F. J. Rodríguez-Fortuño, F. Nori, and A. V. Zayats, "Spin-orbit interactions of light," *Nat. Photonics* **9**, 796–808 (2015).
- K. Y. Bliokh and F. Nori, "Spatiotemporal vortex beams and angular momentum," *Phys. Rev. A* **86**, 033824 (2012).
- K. Y. Bliokh, A. Y. Bekshaev, and F. Nori, "Optical momentum, spin, and angular momentum in dispersive media," *Phys. Rev. Lett.* **119**, 073901 (2017).
- M. F. Picardi, K. Y. Bliokh, F. J. Rodríguez-Fortuño, F. Alpegiani, and F. Nori, "Angular momenta, helicity, and other properties of dielectric-fiber and metallic-wire modes," *Optica* **5**, 1016–1026 (2018).
- M. J. Padgett, J. Courtial, and L. Allen, "Light's orbital angular momentum," *Phys. Today* **57**(5), 35–40 (2004).
- S. Franke-Arnold, L. Allen, and M. J. Padgett, "Advances in optical angular momentum," *Laser Photonics Rev.* **2**, 299–313 (2008).
- Z. Qiao, Z. Wan, G. Xie, J. Wang, L. Qian, and D. Fan, "Multi-vortex laser enabling spatial and temporal encoding," *PhotonIX* **1**, 13 (2020).
- J. Courtial, K. Dholakia, D. A. Robertson, L. Allen, and M. J. Padgett, "Measurement of the rotational frequency shift imparted to a rotating light beam possessing orbital angular momentum," *Phys. Rev. Lett.* **80**, 3217–3219 (1998).
- M. J. A. Padgett, "A new twist on the Doppler shift," *Phys. Today* **67**(2), 58–59 (2014).
- M. J. Padgett, "The mechanism for energy transfer in the rotational frequency shift of a light beam," *J. Opt. A: Pure Appl. Opt.* **6**, S263–S265 (2004).
- A. Belmonte and J. P. Torres, "Optical Doppler shift with structured light," *Opt. Lett.* **36**, 4437–4439 (2011).
- H. Zhou, D. Fu, J. Dong, P. Zhang, and X. Zhang, "Theoretical analysis and experimental verification on optical rotational Doppler effect," *Opt. Express* **24**, 10050–10056 (2016).
- L. Fang, M. J. Padgett, and J. Wang, "Sharing a common origin between the rotational and linear Doppler effects," *Laser Photonics Rev.* **11**, 1700183 (2017).
- F. Lin, L. Hong, Y. Ren, X. Qiu, and L. Chen, "Computational ghost rotational Doppler metrology," *Phys. Rev. Appl.* **19**, 034042 (2023).
- M. Cromb, G. M. Gibson, E. Toninelli, M. J. Padgett, E. M. Wright, and D. Faccio, "Amplification of waves from a rotating body," *Nat. Phys.* **16**, 1069–1073 (2020).
- Q. Wang, Z. Zhou, D. Liu, H. Ding, M. Gu, and Y. Li, "Acoustic topological beam nonreciprocity via the rotational Doppler effect," *Sci. Adv.* **8**, eabq4451 (2022).
- C. Zhang, X. Jiang, J. He, Y. Li, and D. Ta, "Spatiotemporal acoustic communication by a single sensor via rotational Doppler effect," *Adv. Sci.* **10**, 2206619 (2023).
- G. Li, T. Zentgraf, and S. Zhang, "Rotational Doppler effect in nonlinear optics," *Nat. Phys.* **12**, 736–740 (2016).
- P. Georgi, C. Schlickriede, G. Li, S. Zhang, and T. Zentgraf, "Rotational Doppler shift induced by spin-orbit coupling of light at spinning metasurfaces," *Optica* **4**, 1000–1005 (2017).
- H. Zhou, D. Fu, J. Dong, P. Zhang, D. Chen, X. Cai, F. Li, and X. Zhang, "Orbital angular momentum complex spectrum analyzer for vortex light based on the rotational Doppler effect," *Light: Sci. Appl.* **6**, e16251.1–e16251.7 (2016).
- L. Fang, Z. Wan, A. Forbes, and J. Wang, "Vectorial Doppler metrology," *Nat. Commun.* **12**, 4186 (2021).

- ²⁸H. Guo, X. Qiu, S. Qiu, L. Hong, F. Lin, Y. Ren, and L. Chen, "Frequency upconversion detection of rotational Doppler effect," *Photonics Res.* **10**, 183–188 (2022).
- ²⁹Z. Cheng, S. Xue, Y. Lou, P. Wan, Z. Ren, J. Ding, X. Wang, and H. Wang, "Rotational Doppler shift tripling via third-harmonic generation of spatially structured light in a quasi-periodically poled crystal," *Optica* **10**, 20–25 (2023).
- ³⁰M. Zhao, X. Gao, M. Xie, W. Zhai, W. Xu, S. Huang, and W. Gu, "Measurement of the rotational Doppler frequency shift of a spinning object using a radio frequency orbital angular momentum beam," *Opt. Lett.* **41**, 2549–2552 (2016).
- ³¹J. Zheng, S. Zheng, Z. Shao, and X. Zhang, "Analysis of rotational Doppler effect based on radio waves carrying orbital angular momentum," *J. Appl. Phys.* **124**, 164907 (2018).
- ³²B. Liu, H. Giddens, Y. Li, Y. He, S. Wong, and Y. Hao, "Design and experimental demonstration of Doppler cloak from spatiotemporally modulated metamaterials based on rotational Doppler effect," *Opt. Express* **28**, 3745–3755 (2020).
- ³³M. P. Lavery, F. C. Speirits, S. M. Barnett, and M. J. Padgett, "Detection of a spinning object using light's orbital angular momentum," *Science* **341**, 537–540 (2013).
- ³⁴C. Rosales-Guzmán, N. Hermosa, A. Belmonte, and J. P. Torres, "Experimental detection of transverse particle movement with structured light," *Sci. Rep.* **3**, 2815 (2013).
- ³⁵C. Rosales-Guzmán, N. Hermosa, A. Belmonte, and J. P. Torres, "Direction-sensitive transverse velocity measurement by phase-modulated structured light beams," *Opt. Lett.* **39**, 5415–5418 (2014).
- ³⁶X. Hu, B. Zhao, Z. Zhu, W. Gao, and C. Rosales-Guzmán, "In situ detection of a cooperative target's longitudinal and angular speed using structured light," *Opt. Lett.* **44**, 3070–3073 (2019).
- ³⁷M. Seghilani, M. Myara, I. Sagnes, B. Chomet, R. Bendoula, and A. Garnache, "Self-mixing in low-noise semiconductor vortex laser: Detection of a rotational Doppler shift in backscattered light," *Opt. Lett.* **40**, 5778–5781 (2015).
- ³⁸K. Otsuka and S. C. Chu, "Spontaneous generation of vortex and coherent vector beams from a thin-slice c-cut Nd:GdVO₄ laser with wide-aperture laser-diode end pumping: Application to highly sensitive rotational and translational Doppler velocimetry," *Laser Phys. Lett.* **14**, 075002 (2017).
- ³⁹S. Qiu, T. Liu, Y. Ren, Z. Li, C. Wang, and Q. Shao, "Detection of spinning objects at oblique light incidence using the optical rotational Doppler effect," *Opt. Express* **27**, 24781–24792 (2019).
- ⁴⁰S. Qiu, X. Zhu, R. Tang, T. Liu, R. Li, and Y. Ren, "Noncoaxial RDE of circular asymmetry optical vortex for rotating axis detection," *Photonics Res.* **10**, 2541–2548 (2022).
- ⁴¹Z. Li, T. Liu, Y. Ren, S. Qiu, C. Wang, and H. Wang, "Direction-sensitive detection of a spinning object using dual-frequency vortex light," *Opt. Express* **29**, 7453–7463 (2021).
- ⁴²Z. Wan, L. Fang, and J. Wang, "Direction-discriminated rotational Doppler velocimetry with circularly polarized vortex beams," *Opt. Lett.* **47**, 1021–1024 (2022).
- ⁴³Y. Zhai, S. Fu, C. Yin, H. Zhou, and C. Gao, "Detection of angular acceleration based on optical rotational Doppler effect," *Opt. Express* **27**, 15518–15527 (2019).
- ⁴⁴A. Belmonte, C. Rosales-Guzmán, and J. P. Torres, "Measurement of flow vorticity with helical beams of light," *Optica* **2**, 1002–1005 (2015).
- ⁴⁵A. Ryabtsev, S. Pouya, A. Safaripour, M. Koochesfahani, and M. Dantus, "Fluid flow vorticity measurement using laser beams with orbital angular momentum," *Opt. Express* **24**, 11762–11767 (2016).
- ⁴⁶D. B. Phillips, M. P. Lee, F. C. Speirits, S. M. Barnett, S. H. Simpson, M. P. J. Lavery, M. J. Padgett, and G. M. Gibson, "Rotational Doppler velocimetry to probe the angular velocity of spinning microparticles," *Phys. Rev. A* **90**, 011801 (2014).
- ⁴⁷X. Chen, G. Xiao, X. Wei, K. Yang, L. Hui, and B. Yao, "Rotation of an optically trapped vaterite microsphere measured using rotational Doppler effect," *Opt. Eng.* **57**, 036013 (2018).
- ⁴⁸W. Zhang, J. Gao, D. Zhang, Y. He, T. Xu, R. Fickler, and L. Chen, "Free-space remote sensing of rotation at the photon-counting level," *Phys. Rev. Appl.* **10**, 044014 (2018).
- ⁴⁹Y. Zhai, S. Fu, J. Zhang, Y. Lv, H. Zhou, and C. Gao, "Remote detection of a rotator based on rotational Doppler effect," *Appl. Phys. Express* **13**, 022012 (2020).
- ⁵⁰Z. Wan, Y. Liang, X. Zhang, Z. Tang, L. Fang, Z. Ma, S. Ramachandran, and J. Wang, "Remote measurement of the angular velocity vector based on vectorial Doppler effect using air-core optical fiber," *Research* **2022**, 9839502.
- ⁵¹A. Anderson, E. Strong, B. Heffernan, M. Siemens, G. Rieker, and J. Gopinath, "Observation of the rotational Doppler shift with spatially incoherent light," *Opt. Express* **29**, 4058–4066 (2021).
- ⁵²T. Charrett, S. W. James, and R. P. Tatam, "Optical fibre laser velocimetry: A review," *Meas. Sci. Technol.* **23**, 032001 (2012).
- ⁵³Z. Wan, Y. Liang, L. Fang, and J. Wang, "Flexible and robust detection of a remotely rotating target using fiber-guided orbital angular momentum superposed modes," in Conference on Lasers and Electro-Optics, OSA Technical Digest, (2020), paper AM1K.1.
- ⁵⁴R. Ismael, T. Lee, B. Oduro, Y. Jung, and G. Brambilla, "All-fiber fused directional coupler for highly efficient spatial mode conversion," *Opt. Express* **22**, 11610–11619 (2014).
- ⁵⁵S. Li, Q. Mo, X. Hu, C. Du, and J. Wang, "Controllable all-fiber orbital angular momentum mode converter," *Opt. Lett.* **40**, 4376–4379 (2015).
- ⁵⁶W. Zhou, H. Cao, and J. Wang, "All-fiber orbital angular momentum (OAM) broadband functional devices for OAM generation and beam splitting in conventional graded-index multimode fiber," in *Asia Communications and Photonics Conference (ACP)* (IEEE, 2018), pp. 1–3.
- ⁵⁷J. Leach, S. Keen, M. J. Padgett, C. Saunter, and G. D. Love, "Direct measurement of the skew angle of the Poynting vector in a helically phased beam," *Opt. Express* **14**, 11919–11924 (2006).
- ⁵⁸A. Q. Anderson, E. F. Strong, B. M. Heffernan, M. E. Siemens, G. B. Rieker, and J. T. Gopinath, "Detection technique effect on rotational Doppler measurements," *Opt. Lett.* **45**, 2636–2639 (2020).
- ⁵⁹M. P. Lavery, S. M. Barnett, F. C. Speirits, and M. J. Padgett, "Observation of the rotational Doppler shift of a white-light, orbital-angular-momentum-carrying beam backscattered from a rotating body," *Optica* **1**, 1–4 (2014).
- ⁶⁰L. Fang, Z. Wan, and J. Wang, "Structured light interferometry," *arXiv:1912.02446v2* (2019).
- ⁶¹Y. Ren, S. Qiu, T. Liu, and Z. Liu, "Compound motion detection based on OAM interferometry," *Nanophotonics* **11**, 1127–1135 (2022).